Chemical Geology 530 (2019) 119323

Contents lists available at ScienceDirect

Chemical Geology

journal homepage: www.elsevier.com/locate/chemgeo

Implications of overstepping of garnet nucleation for geothermometry, geobarometry and P–T path calculations

Frank S. Spear*, Oliver M. Wolfe

Department of Earth and Environmental Sciences, Rensselaer Polytechnic Institute, 110 8th Street, Troy, NY, 12180, United States

ARTICLE INFO

Editor: Balz Kamber

Keywords:
Garnet
Nucleation
P–T paths
Overstepping
Thermobarometry
Effective bulk composition

ABSTRACT

The composition of a porphyroblast such as garnet is not governed by equilibrium relations when it nucleates and grows after considerable overstepping. The approach followed here is to assume the composition is controlled by the maximum driving force (MDF) or parallel tangent model and to examine the potential pitfalls for assuming equilibrium. The MDF model ensures Fe-Mg partitioning equilibrium between the matrix phases and growing porphyroblast, but the net transfer equilibrium controlling grossular content has a different stoichiometry from the equilibrium relations. An important result of this study is that garnet zoning profiles generated using this model and assuming chemical fractionation are nearly identical to zoning profiles grown assuming continuous equilibrium and it is impossible to discern whether garnet grew under near-equilibrium conditions or only after considerable overstepping by examination of the zoning profile alone.

Pressure–temperature paths calculated using the method of intersecting isopleths from simulations in which garnet was grown after overstepping and assuming the MDF model typically display nearly isothermal loading or loading with minor heating paths, even when the garnet was grown under isothermal and isobaric conditions. Garnet-plagioclase barometry on the garnet core and rim also suggests loading during garnet growth, even for crystals grown isothermally and isobarically. Garnet-biotite Fe-Mg exchange thermometry does, however, recover the correct temperature to within 10 °C for both the garnet core and rim.

Comparison of natural samples to the theoretical calculations suggests that the local effective bulk composition in the vicinity of garnet is depleted in Na_2O, in addition to FeO, MnO and CaO, thus rendering calculation schemes that rely on knowledge of the bulk composition difficult to administer. To the extent that garnet has nucleated and grown after considerable overstepping, application of methods of extracting P–T paths from the chemical zoning in garnet will yield incorrect results if those methods assume continuous equilibration with the matrix. The major discrepancy comes from calculation of the P–T conditions of the garnet core. Simulations and natural samples suggest that under typical scenarios the garnet rim is in near equilibrium with the matrix assemblage so equilibrium approaches (thermobarometry or intersecting isopleths) should recover the peak metamorphic conditions with reasonable assuredness.

1. Introduction

A mainstay of modern metamorphic petrology is the use of equilibrium calculations to infer the conditions of metamorphism and metamorphic P–T paths. However, recent advances utilizing a method that is independent of the assumption of equilibrium — specifically, quartz in garnet or QuiG barometry — reveals that the nucleation and growth of garnet and presumably other porphyroblasts does not occur under near equilibrium conditions but rather occurs only after considerable overstepping of the equilibrium garnet isograd reaction (Hollister, 1969; Waters and Lovegrove, 2002; Wilbur and Ague, 2006; Pattison and Tinkham, 2009; Pattison et al., 2011; Spear et al., 2014; Spear, 2017; Castro and Spear, 2016; Wolfe and Spear, 2018). Garnet growth is therefore controlled at least in part by kinetics, and equilibrium calculations applied to such a system may yield incorrect estimates of P–T conditions and paths.

This paper explores some aspects of the issues surrounding the use of equilibrium calculations to the estimate of P–T conditions involving garnet. These include (a) knowledge of the effective bulk composition (EBC) during the growth of garnet — a necessary condition for the application of mineral assemblage diagrams (MADs) or pseudosections; (b) elucidation of the governing equations for growing a porphyroblast after overstepping of several tens of degrees and/or several kilobars pressure; (c) exploration of the non-uniqueness of garnet zoning profiles

* Corresponding author.
E-mail address: spearf@rpi.edu (F.S. Spear).

https://doi.org/10.1016/j.chemgeo.2019.119323
Received 18 June 2019; Received in revised form 25 September 2019; Accepted 28 September 2019
Available online 15 October 2019
0009-2541/ © 2019 Elsevier B.V. All rights reserved.

with respect to evaluating the appropriate governing equations for porphyroblast growth; (d) examining the implications of applying equilibrium calculations to the interpretation of garnet zoning profiles; and (e) exploration of the accuracy of equilibrium geothermobarometry in light of overstepped metamorphic reactions.

2. Results from the application of QuiG barometry

The arguments presented in Spear et al. (2014) and Spear and Wolfe (2018) based on the application of quartz-in-garnet (QuiG) barometry strongly support the interpretation that garnet nucleated only after considerable overstepping. The P–T conditions of garnet nucleation for those samples have been inferred from a combination of QuiG barometry, zirconium-in-rutile (ZiR) thermometry when possible, and regional P–T conditions based on isograd sequences and phase equilibrium calculations of peak metamorphic conditions.

However, many of the samples studied by Spear and Wolfe (2018), when evaluated using the method of intersecting isopleths and assuming that the measured bulk rock composition (the OBC or original bulk composition of Spear and Wolfe, 2018), have garnet core compositions that plot very near the equilibrium garnet-in isograd. This result is not uncommon in numerous recent publications (e.g. Tinkham and Ghent, 2005a; Gaidies et al., 2006, 2008; Dragovic et al., 2012; Moynihan and Pattison, 2013; George and Gaidies, 2017; Lanari and Duesterhoeft, 2019), raising the question of whether garnet did, in fact, nucleate very close to this equilibrium isograd.

Although the results of QuiG barometry suggest that garnet does not nucleate at or very near the calculated equilibrium isograd, the possibility exists that the thermodynamic data are insufficiently accurate to calculate the precise location of the isograd. As an exercise, it is possible to make adjustments to the enthalpy of the spessartine component in garnet so that the intersecting isopleths for the garnet core align nearly exactly on the equilibrium garnet isograd. This experiment has been conducted for one of the samples studied by Spear and Wolfe (2018) and the results shown in Fig. 1. The original H_{sps} value of −5,641,080 J/mol (following Berman, 1988, 1990) was adjusted to a value of −5,625,000 J/mol (an increase of 16,080 J/mol or 0.28%) so that the spessartine isopleth lined up exactly on the isograd. Coincidentally, almandine and grossular also intersect the isograd at very nearly the same P–T conditions. However, pyrope and, consequently, Fe/(Fe + Mg) plot 20 and 30 °C higher, respectively. Therefore, no modification of the enthalpy of a single garnet component can align all

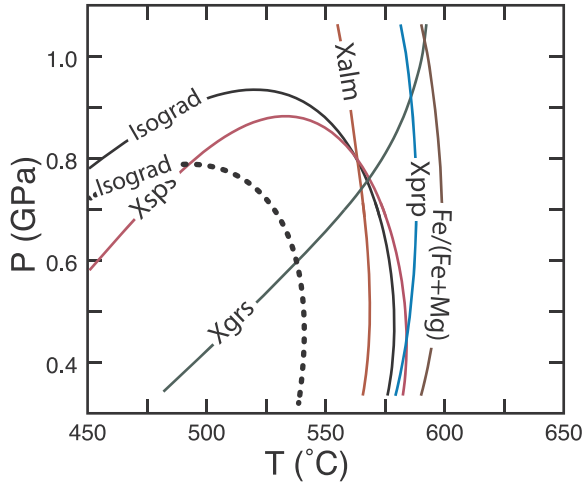

Fig. 1. P–T diagram showing the intersecting garnet isopleths for sample TM-626 with H_{sps} adjusted so that the spessartine isopleth falls exactly on the garnet isograd at 565 °C, 0.8 GPa. Labels identify the isograd and isopleths for garnet components. The garnet isograd calculated with the unmodified H_{sps} is shown as a dotted line.

of the garnet core isopleths. Additionally, this experiment has only been conducted on a single sample, and it is not likely that the same adjustment of spessartine enthalpy would serve to align garnet core isopleths in other samples, simply based on the observed discrepancy between published isograds and isopleth intersections. The same experiment conducted using HP11 ds6.2 (Holland and Powell, 2011; White et al., 2014a, b) results in a required change in spessartine enthalpy from the original value of −5,693,490 J/mol (from Dachs et al., 2009) to −5,659,000 J/mol, an increase of 34,490 J/mol or 0.6%. Considering the magnitude of error associated with H_{sps} from Dachs et al. (2009) of only ± 1400 J/mole, it does not seem reasonable that H_{sps} could be off by 16–34 kJ/mol.

Ultimately, then, evaluation of the P–T conditions of garnet core growth, and consequently of the EBC controlling garnet core composition, hinges on whether the method of intersecting isopleths or QuiG barometry provide a more accurate estimate of P and T.

The accuracy of QuiG barometry has been verified experimentally and Thomas and Spear (2018) have concluded that QuiG barometry is capable of reproducing the experimental conditions in which quartz inclusions were encapsulated in garnet to better than 10% of the known experimental pressure. However, it is possible that application of the experimental results to natural samples might neglect some important process that might modify the internal pressure of a quartz inclusion. Although a number of post-entrapment processes might serve to decrease the inclusion pressure, no process has yet been proposed that would result in an increase in inclusion pressure. We therefore assume that the QuiG barometry provides an accurate assessment of the pressure of garnet nucleation, as has been concluded by Ashley et al. (2014); Spear et al. (2014); Castro and Spear (2016); Wolfe and Spear (2018); Spear and Wolfe (2018); Dragovic et al. (2012), and Thomas and Spear (2018). Supplemented with zirconium-in-rutile or regional P–T considerations, the results of QuiG barometry can be used to infer the P–T conditions of initial garnet growth. The ability of QuiG to preserve these conditions through a metamorphic episode will be addressed in the discussion section.

3. Thermodynamic considerations

The purpose of this next section is to provide a generalized approach to the development of the equations used to calculate the composition of a phase growing out of equilibrium and towards that end a short review of the equilibrium relations is warranted. As is well-known, application of thermodynamics to the calculation of equilibrium phase relations requires solving the system of equations for the assemblage in question of the form

$$0 = \sum \nu_i \mu_i \quad (1)$$

where μ_i is the chemical potential of the ith phase component and ν_i is the stoichiometric coefficient of the phase component in the equation. For example, the relationship

$$0 = 3\mu_{prp}^{Grt} - 4\mu_{qtz}^{Qtz} - \mu_{clinochlore}^{Chl} - \mu_{amesite}^{Chl} + 8\mu_{H2O}^{Fluid}$$

is one such equation governing the composition of garnet growing from chlorite in a pelitic schist. Given a system of n_{sys} system components with a total of p phases and n_{ph} independent phase components, there are n_{ph}-n_{sys} such relationships as well as a stoichiometric relationship for each p phase. The difference between the number of unknowns (n_{ph} + 2) and equations (n_{ph}-n_{sys} + p) is the phase rule variance (v = n_{sys} + 2 – p).

If mass balance constraints are desired, then there are an additional n_{sys} mass balance equations and an additional p unknowns representing the amounts of each phase. The variance of the full equilibrium system at constant bulk composition is thus v = n_{sys} + 2 – p – n_{sys} + p = 2, which is Duhem's theorem (see Spear, 1993 for detailed derivations).

An algorithm for determining a linearly independent set of

equations such as Eq. (1) was presented by Thompson (1982). The algorithm involves performing a Gaussian reduction on a n_{ph} x n_{sys} matrix that defines the composition of each phase component in terms of the system components. An identical reduction is performed on an n_{ph} x n_{ph} identity matrix. The Gaussian reduction results in the last $n_{ph} - n_{sys}$ rows being all zeros. The same rows in the identity matrix after identical row reductions are the set of so-called null space reactions. That is, the set of linearly independent reactions among the phase components which, when written in terms of chemical potentials, take the form of Eq. (1).

In a system out of equilibrium, it is necessary to make assumptions about the governing energetics in order to make calculations of the phase compositions and system evolution. Following Hillert (2008; see also Thompson and Spaepen, 1983) we adopt a method that we call the maximum driving force (MDF) method (also known as the parallel tangent method; Gaidies et al., 2011). The basic premise of this approach is that the system will follow a path that results in the maximum decrease in free energy. As demonstrated by Thompson and Spaepen (1983) and discussed by Pattison et al. (2011), Spear et al. (2014), and Spear and Pattison (2017), this method predicts that the composition of the out of equilibrium phase that will form is that which lies on a tangent plane that is parallel to the tangent plane for the equilibrated phases. Mathematically, the parallel tangent is defined by equations such as

$$\mu_{alm}^{Grt} - \mu_{prp}^{Grt} = \mu_{alm}^{Matrix} - \mu_{prp}^{Matrix} \quad (2a)$$

$$\mu_{sps}^{Grt} - \mu_{prp}^{Grt} = \mu_{sps}^{Matrix} - \mu_{prp}^{Matrix} \quad (2b)$$

$$\mu_{grs}^{Grt} - \mu_{prp}^{Grt} = \mu_{grs}^{Matrix} - \mu_{prp}^{Matrix} \quad (2c)$$

where garnet is the phase out of equilibrium and the term μ_{alm}^{Matrix} refers to the chemical potential of the almandine component as defined by the chemical potentials of matrix phases. Inasmuch as equations (2) are differences, then number of independent relations of the form of (2) is equal to the number of independent components in the phase of interest (three for garnet).

Calculation of the independent set of relations of form (2) can readily be accomplished by further manipulation of the system of linearly independent relations determined from the Gaussian reduction described above. The method is to simply subtract the appropriate equations until they take the proper form. For example, Table 1 shows the set of stoichiometric relations in the MnNCKFMASH system containing the phases quartz + muscovite + plagioclase + fluid + biotite + chlorite + garnet for the equilibrium relations (1). If garnet nucleates and grows out of equilibrium, however, the last four equations are not valid and must be replaced by the MDF equations (2). These equations are readily derived by successively subtracting the equation that defines the pyrope component (the 9th row) from last three equations (Table 2). It will be noted in Table 2 that the first two MDF equations are exchange reactions that describe the Fe-Mg and Mn-Mg exchange between garnet and the matrix assemblage. The third equation is a net transfer reaction (Grs – Prp). Note that the number of MDF equations for garnet (Table 2) is one fewer than the number of equilibrium relations for garnet (Table 1). This is always true. Therefore, there is one additional degree of freedom introduced for each phase that obeys the MDF relations. For a system under mass balance constraints, Duhem's theorem becomes V = 2 + number of MDF phases. That is, the system is no longer defined simply by two independent variables such as P and T, but the value of additional variable need be specified. A logical choice is the amount of a phase (in particular, the out-of-equilibrium phase), the growth of which will be limited by kinetics. The system of MDF equations can be constructed for any number of phases out of equilibrium and can be solved at constant P and T if the amounts of the phases out of equilibrium is specified, either by a kinetic formulation or by simply specifying an amount.

4. Calculation of effective bulk composition (EBC)

4.1. Method for calculation of EBC

Using the above equations for the MDF model, the composition of the core of an overstepped garnet can be calculated and the result will be a function of the pressure, temperature, and effective bulk composition (EBC) at the time of its formation. If the P–T conditions and composition of the garnet core are known, then the EBC that yields the measured garnet core composition can be calculated, as was developed and applied by Spear and Wolfe (2018). The method involves solving the additional independent equations

$$0 = (X_{alm,Meas} - X_{alm,Calc}) \quad (3a)$$

$$0 = (X_{sps,Meas} - X_{sps,Calc}) \quad (3b)$$

$$0 = (X_{grs,Meas} - X_{grs,Calc}) \quad (3c)$$

by varying the MnO, CaO and FeO or MgO amounts in the bulk composition.

All calculations have been performed using a module in Program Gibbs that solves Eqs. (1) using the constraints from equations 2 and 3. In order to assess the possible biases from the choice of thermodynamic data sets, calculations have been done using the SPaC dataset (Spear and Pyle, 2010), the Holland and Powell (2011) dataset ds6.2 with activity models as updated in White et al. (2014a, b) and the Holland and Powell (1998) dataset ds5.5 with activity models as described by Pattison and DeBuhr (2015).

4.2. Results of calculated EBC

Spear and Wolfe (2018) discussed the results of calculations of the effective bulk composition (EBC) based on the method described above

Table 1
Stoichiometric coefficients for the linearly independent set of reactions among the phases quartz + muscovite + plagioclase + fluid + biotite + chlorite + garnet in the system MnNCKFMASH.

abQz	H2O	Mg-C	Fe-C	Ms	Ab	An	Clin	Mg-A	Daph	Fe-A	MnCh	Phlo	East	Anni	Side	MnBi	Prp	Alm	Sps	Grs
0	0	5	−5	0	0	0	−1	0	1	0	0	0	0	0	0	0	0	0	0	0
0	0	5	−4	−1	0	0	−1	0	0	1	0	0	0	0	0	0	0	0	0	0
0	0	1	0	−1	0	0	−1	1	0	0	0	0	0	0	0	0	0	0	0	0
2.333	1.333	−1.333	0	0.333	0	0	−0.333	0	0	0	0	1	0	0	0	0	0	0	0	0
2.333	1.333	−0.333	0	−0.667	0	0	−0.333	0	0	0	0	0	1	0	0	0	0	0	0	0
2.333	1.333	1.667	−3	0.333	0	0	−0.333	0	0	0	0	0	0	1	0	0	0	0	0	0
2.333	1.333	1.667	−2	−0.667	0	0	−0.333	0	0	0	0	0	0	0	1	0	0	0	0	0
2.333	1.333	−1.667	0	0.667	0	0	0.333	0	0	0	−0.667	0	0	0	0	1	0	0	0	0
−1.333	2.667	0.333	0	−0.333	0	0	−0.667	0	0	0	0	0	0	0	0	0	1	0	0	0
−1.333	2.667	3.333	−3	−0.333	0	0	−0.667	0	0	0	0	0	0	0	0	0	0	1	0	0
−1.333	2.667	0	0	0	0	0	0	0	0	0	−0.667	0	0	0	0	0	0	0	1	0
3.667	−1.333	−1.667	0	1.667	0	−3	0.333	0	0	0	0	0	0	0	0	0	0	0	0	1

Table 2
MDF equations assuming that garnet is the only phase that has grown out of equilibrium with the matrix.

abQz	H2O	Mg-C	Fe-C	Ms	Ab	An	Clin	Mg-A	Daph	Fe-A	MnCh	Phlo	East	Anni	Side	MnBi	Prp	Alm	Sps	Grs
0	0	3	−3	0	0	0	0	0	0	0	0	0	0	0	0	0	−1	1	0	0
0	0	−0.333	0	0.333	0	0	0.667	0	0	0	−0.667	0	0	0	0	0	−1	0	1	0
5	−4	−2	0	2	0	−3	1	0	0	0	0	0	0	0	0	0	−1	0	0	1

Table 3
Calculated EBC for sample TM-626 using different thermodynamic databases at the inferred nucleation conditions of 575 °C, 10,750 bars (wt.% oxides).[1].

	OBC[1]	EBC[2] SPaC18	EBC[2] HP98 ds5.5	EBC[2] HP11 ds6.2
SiO_2	55.72			
Al_2O_3	16.16			
MgO	3.97			
FeO	10.76	7.52	9.01	10.57
MnO	0.44	0.16	0.07	0.10
CaO	0.64	0.23	0.55	0.20
Na_2O	1.25			
K_2O	4.05			
H_2O	10.00			

[1] Original bulk composition (OBC) were determined from integration of scans using the electron microprobe of thin sections.
[2] Effective bulk composition (EBC) calculated for selected elements as described in the text.

based on the MDF. In this paper, the results for a single sample (TM-626) are investigated in more detail to determine the extent to which the differences between the original bulk composition (OBC) and calculated EBC depend on the choice of thermodynamic data bases.

Table 3 shows the calculated results for sample TM-626 using the SPaC18, HP98 ds5.5, and HP11 ds6.2 databases using the components FeO, MnO and CaO as monitors. All three sets of calculations reveal that the EBC is depleted in MnO and CaO relative to the OBC, although the amount varies between datasets. The EBC is also depleted in FeO using both the SPaC18 and HP98 databases, but the depletion is negligible using the HP11 database.

Results from calculations on the eight samples discussed by Spear and Wolfe (2018) are plotted in Fig. 2. All samples require EBCs that are depleted in MnO and have a lower Fe/Mg than the measured bulk composition. CaO is also depleted in epidote-free samples but shows both depletion and enrichment in epidote-bearing samples.

4.3. Models for EBC

Knowledge of the EBC during garnet growth is obviously critical for methods that require mass balance for the determination of P–T conditions. A number of papers have discussed this issue and a thorough analysis of the uncertainties in P–T estimates based on uncertainties in the EBC was presented by Palin et al. (2016). The three main methods in common use for determination of rock compositions are whole-rock XRF analyses, calculation of the rock composition using modal analysis and mineral compositions, and whole rock analysis of a portion of a thin section by scanning EDS analysis. The XRF method tends to average compositional heterogeneities in a sample whereas the other two methods are highly dependent on the amounts of the minerals present in the analyzed thin section. Palin et al. (2016) and Lanier and Duesterhoeft (2019) have presented insightful discussions of the criticality of inferring the correct EBC, regardless of the method employed.

Unfortunately, none of these methods of determining rock composition can *a priori* determine the effective bulk composition during garnet growth. Methods based on XRF analyses, while providing precise chemistry, cannot readily distinguish the effective bulk composition in which local equilibrium was attained, especially in a rock with subtle but important compositional layering. Thin section-based methods suffer from the significant concern that the thin section might not contain the required representative modal distribution of phases. Lanier and Duesterhoeft (2019; see also Tinkham and Ghent, 2005b) have developed sophisticated software (XMapTools and Bingo-Antidote) that allows the user to readily calculate rock compositions based on the choice of volume of equilibration in composition maps of the sample, and it is even possible to exclude the interior of phases that are chemically zoned or phases that incorporate some major elements but are not being considered in the analysis (e.g. tourmaline – see also Figs. 2 and 3 of Palin et al., 2016). However, the results of the above calculations (Fig. 2 and Table 3) and those in Spear and Wolfe (2018) indicate that no amount of manipulation of the modal amounts of phases can accurately reproduce the EBC for the sample during garnet growth.

In order to gain insight into the controls on the EBC during porphyroblast growth, it is necessary to review the possible kinetic limitations. Broadly, there are two possible rate-limiting processes that can control the rate of porphyroblast growth and the EBC: surface processes and transport. Surface processes include the energetics of breaking down phases that are being consumed and those involved with the formation of a new phase. Although no quantitative assessment of these

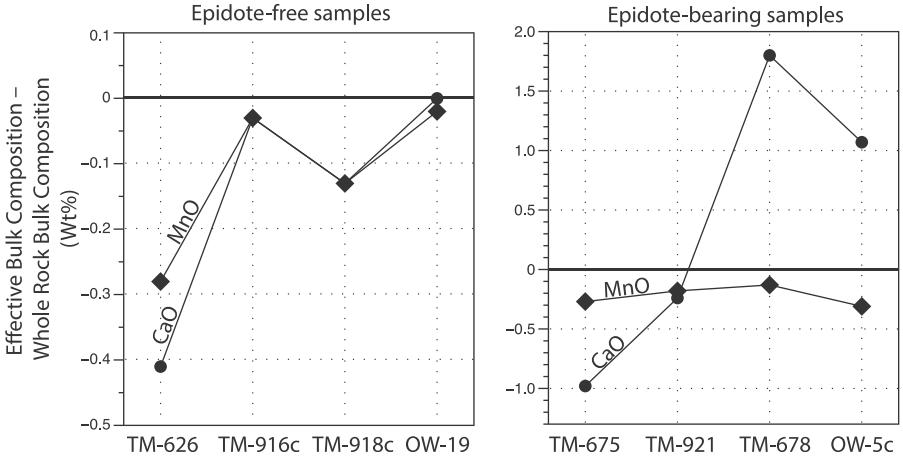

Fig. 2. Plots showing the results of calculations of the effective bulk composition (EBC) for the eight samples examined by Spear and Wolfe (2018). Symbols show the inferred EBC relative to the whole-rock measured bulk composition (at a value of 0). Note that MnO is always lower than the measured MnO content for all sample studied. Calculated with the SPaC (Spear and Pyle, 2010) dataset.

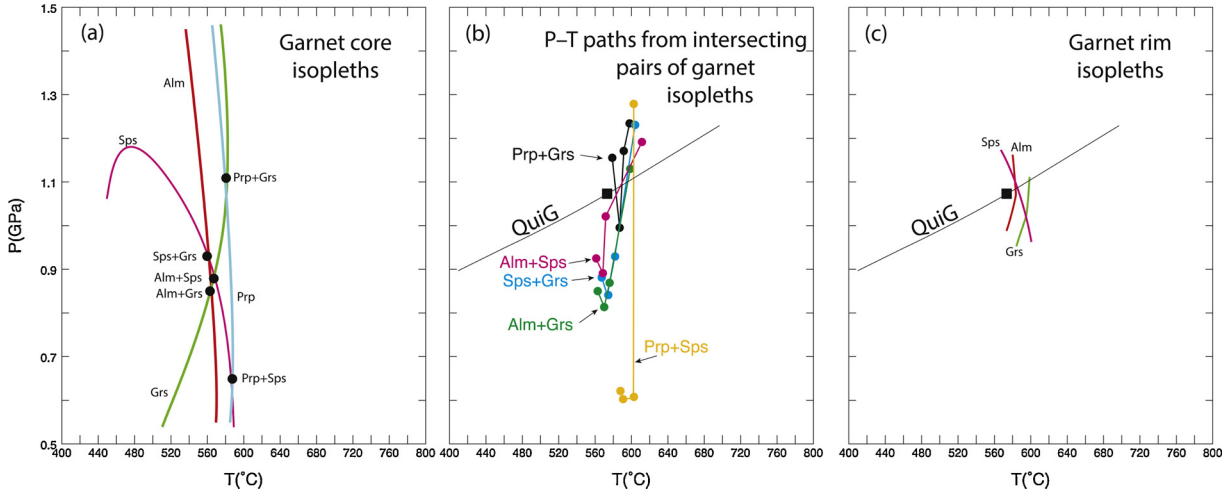

Fig. 3. P–T diagrams showing inferred P–T paths for sample TM-626 using the method of intersecting isopleths. (a) Contours for pyrope (prp), almandine (alm), spessartine (sps), and grossular (grs). The black dots show the intersections of each pair of isopleths and might be used to infer the P–T conditions of the garnet core. (b) P–T paths inferred from different pairs of isopleths (color coded). The line labeled QuiG is the quartz-in-garnet Raman barometer and the inferred P–T conditions for garnet nucleation and growth are indicated by the black square. Note that the P–T paths are similarly shaped, but all imply isothermal loading whereas the garnet is interpreted to have grown at constant P–T (Wolfe and Spear, 2017; Spear and Wolfe, 2018). (c) Isopleths of almandine, spessartine, and grossular for the garnet rim. The similarity of these intersections with the black square suggest an approach to equilibrium at the peak of metamorphism.

processes for metamorphic rocks is available, it is probable that the kinetics of breaking down reactant phases is more inhibitive than those involved with growing an existing phase. Transport process include transport through the grain boundary medium (grain boundary diffusion) and transport within existing phases (lattice diffusion). It is well-know that the rates lattice diffusion in silicates is highly variable and at any set of external conditions it is likely that some elements in certain phases will be highly mobile whereas others will be essentially immobile (e.g. Carlson, 2002). Thus, it is likely that lattice diffusion plays a significant role in affecting some aspects of the effective bulk composition. It is similarly likely that grain boundary diffusion is highly variable for different elements under different conditions. For example, Carmichael (1969) argued for the immobility of Al to explain common metamorphic textural associations and Carlson (1989, 1991) has argued for the diffusivity of Al to be rate-limiting in garnet growth.

A quantitative analysis of the factors affecting the EBC is beyond the scope of this paper, but it is worth reiterating that there is currently no model that will permit accurate *a priori* prediction of the EBC and how it evolves during recrystallization.

5. Impact of the choice of assumed thermodynamic models on calculated P–T paths

A method common to many recent publications is to use what has been referred to as the method of intersecting isopleths (MII) (e.g. Moynihan and Pattison, 2013; Gaidies et al., 2015; Dragovic et al., 2012; George and Gaidies, 2017; St-Onge and Davis, 2017; see discussion in Lanari and Duesterhoeft, 2019). There are four variable compositional parameters in typical pelitic garnets, the intersection of any two of which will define a point in P–T space. These intersections have been interpreted as points through which the rock has passed and the array as defining the rock P–T path. Calculation of the P–T conditions of an isopleth of garnet composition requires an assumption about the effective bulk composition throughout the duration of garnet growth as well as assumptions about appropriate equations governing the composition of garnet (equilibrium versus non-equilibrium). As discussed in the previous section, the EBC is effectively un-knowable from first principles, so this effort is fraught with uncertainty. Equally impactful is the choice of models for the growth of garnet. As discussed in the section on thermodynamic considerations, the equilibrium model involves solving a set of equations of the form of Eq. (1) whereas garnet that is nucleating and growing out of equilibrium is governed by a set of equations similar to (2). The equilibrium Eqs. (1) ensure both partitioning and net-transfer equilibrium is maintained whereas the MDF equations (2) ensure Fe-Mg partitioning equilibrium is maintained but the net transfer equilibrium between grossular and the matrix assemblage has a different stoichiometry from the equilibrium relation.

To explore the impact of choice of models, a series of calculations have been done on the measured garnet zoning profile for sample TM-626 and presented as inferred P–T paths (Figs. 3–5). The various models are these:

(1) Application of the method of intersecting isopleths on the measured zoning profile of a garnet assuming the whole rock (measured) bulk composition is constant throughout (Fig. 3a and b).
(2) Application of the method of intersecting isopleths on the garnet rim composition assuming a bulk composition similar to (1) but in which garnet has been removed (the garnet-free whole rock bulk composition) (Fig. 3c).
(3) Calculation of a synthetic garnet zoning profile at constant P–T conditions (isothermal and isobaric) using the MDF constraints (equations 2) and application of the method of intersecting isopleths on this synthetic zoning profile (Fig. 4).

In all of these models, the method of intersecting isopleths has been applied by making the assumption that the entire system has equilibrated at every pressure and temperature.

5.1. Model results

The isopleths for garnet core composition shown in Fig. 3a (Model 1) do not all intersect in a single point, which they should if all of the assumptions are met and the thermodynamic data and activity models are correct. Isopleths for almandine, spessartine, and grossular intersect in a fairly small triangle around 0.9 GPa and these are often the isopleths used in the MII. However, the isopleth for pyrope falls approximately 30 degrees higher; it intersects the spessartine isopleth at around 0.65 GPa, the grossular isopleth at around 1.1 GPa and the almandine and pyrope isopleths do not intersect at all. A number of studies have used the close intersections of the almandine, spessartine and grossular isopleths as indication of near-equilibrium crystallization; however, the disparity of those isopleths with that for pyrope renders

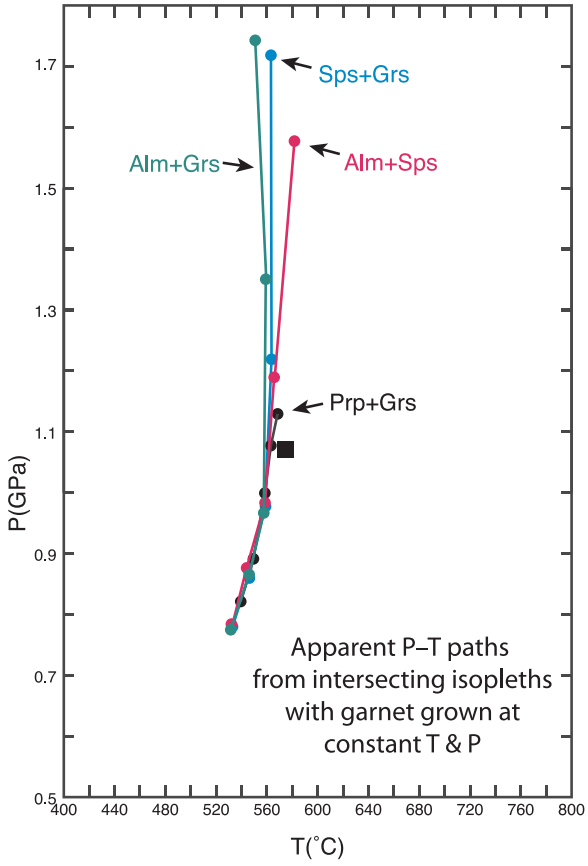

Fig. 4. P–T paths inferred from the method of intersecting isopleths (similar to Fig. 3) from a simulated garnet zoning profile grown at 575 °C, 1.075 GPa (the black square) following the method described by Spear (2017). Note that the intersecting isopleths all imply isothermal loading even though the garnet was grown at constant P and T.

this conclusion suspect.

In Fig. 3b are shown four P–T paths based on the core-rim garnet zoning. All paths are generally similar and suggest an increase in P and T during garnet growth. It should be noted, however, that paths based on almandine-pyrope intersections would not plot on the diagram and paths based on pyrope-spessartine, although ending at P–T conditions similar to the other paths, suggest pressure for the garnet core was significantly lower.

The results of Model 2 are shown in Fig. 3c. As can be seen, the estimated P–T conditions for the garnet rim using a garnet-absent bulk composition are 0.1-0.2 GPa lower than those inferred for the garnet rim assuming a constant (unfractionated) bulk composition (Fig. 3b), again emphasizing the first-order impact of assumptions about the bulk composition on inferred P–T conditions. It is also worth noting that the Model 2 isopleths are within uncertainty of the P–T conditions estimated for this sample by Spear and Wolfe (2018: 575 °C, 1.075 GPa) which provides reasonable surety that the rim of the garnet formed in near-equilibrium conditions and that the thermodynamic data are capable of reproducing these conditions.

The synthetic garnet zoning profile (Model 3) is nearly identical to that presented by Spear (2017, Fig. 2 of that paper). P–T paths inferred from intersecting isopleths from this synthetic zoning profile (Fig. 4) all show dramatic increases in pressure (0.3 to 0.9 GPa) over modest increases in temperature (530–580 °C). However, the synthetic garnet was grown under isothermal, isobaric conditions (indicated by the square in Fig. 4). This example should illustrate beyond any doubt that the P–T conditions inferred from garnet zoning are dependent to a first order on the assumptions made in attempting to recover the P–T history.

It is tempting to believe the paths calculated from zoned garnet assuming the phase crystallized under near-equilibrium conditions is correct because these paths generally conform to preconceived notions of prograde paths for Barrovian facies series. However, it must be acknowledged that very similar paths are calculated when garnet grows under isothermal, isobaric conditions following the MDF criteria. It is thus unfortunate, but nevertheless true, that the chemical zoning in garnet does not contain information about the prograde P–T path if the results of QuiG barometry are correct and the garnet nucleated and grew after considerable overstepping.

As an additional example, consider the P–T paths inferred from garnet zoning from a suite of samples from the Wopmay Orogen (St-Onge and Davis, 2017). An isothermal, isobaric simulation was run for sample C408 using the same methods as above at the calculated peak P–T conditions of 600 °C, 0.4 GPa and the model garnet zoning is displayed in Fig. 5. Comparison with Fig. 8b of St-Onge and Davis (2017) reveals the zoning profiles to be virtually identical with Ca relatively flat, Mg increasing slightly, Mn decreasing in a typical bell-shape, and

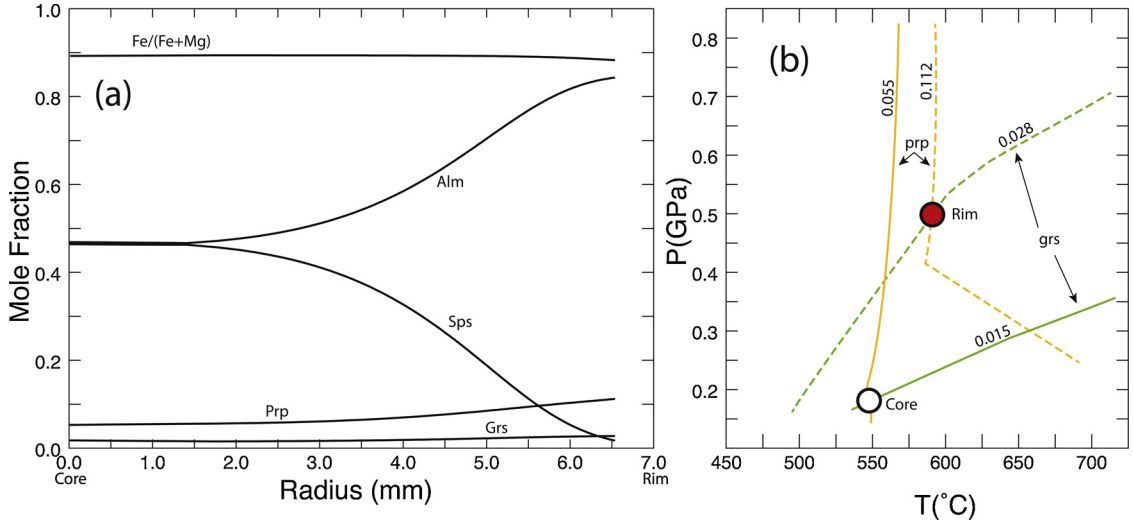

Fig. 5. (a) Calculated garnet zoning profile using the MDF model and isothermal, isobaric growth at 600 °C, 0.4 GPa using the bulk composition for sample C408 from St-Onge et al. (2018). (b) P–T diagram contoured with isopleths of pyrope and grossular for the garnet core (solid lines) and rim (dashed lines) shown in (a). Note the inferred P–T path of increasing P and T even though the garnet was grown isothermally and isobarically.

almandine increasing towards the rim. Using the MDF calculated garnet core and rim compositions from the simulation, Fig. 5b shows how the isopleths for Mg and Ca plot in P–T space. The core intersection occurs at around 550 °C, 0.16 GPa whereas the rim isopleths intersect at around 600 °C, 0.5 GPa. That is, the P–T path that would be deduced from applying equilibrium isopleth calculations for a garnet grown isothermally and isobarically is one of increasing pressure and temperature, just as was inferred by St-Onge and Davis (2017). However, this inference for the model simulation is clearly incorrect and it must be concluded that isothermal, isobaric growth of sample C408 from this study is also consistent with the observed mineral zoning.

6. Thermobarometry in the context of overstepping

Application of equilibrium thermobarometers involving garnet need to be reevaluated in light of the possibility that the composition of garnet may not be controlled by equilibrium relations (i.e. Eqs. 1) but rather by the MDF equations (i.e. Eqs 2). To evaluate the degree to which equilibrium thermobarometers may yield spurious results, two sets of calculations have been conducted and compared. An equilibrium mineral assemblage diagram (MAD or pseudosection) was calculated in the MnNCKFMASH system considering only the phases garnet – chlorite – muscovite – biotite – quartz – plagioclase – fluid in order to avoid over complication of the diagram (Fig. 6). Phase compositions at 600 °C, 1 GPa are presented in Table 4. Three fields are represented (all with muscovite + quartz + H_2O): chlorite + biotite + plagioclase, chlorite + biotite + garnet + plagioclase, and biotite + garnet + plagioclase. The composition of all phases was calculated at every P and T and the value of the distribution constant

$$K_D = \frac{(Fe/Mg)_{Grt}}{(Fe/Mg)_{Bt}}$$

contoured on the P–T diagram (Fig. 6a: black lines). A second MAD was calculated in which garnet was excluded from the calculations so that the entire diagram incorporated only the assemblage chlorite + biotite + plagioclase + muscovite + quartz + H_2O. The composition of garnet at each P–T point was calculated using the MDF equations (Eqs. 2) and the K_D for garnet-biotite calculated and contoured on the P–T diagram (Fig. 6a: red lines). The results show very similar contours for each model (black lines versus red lines in Fig. 6a) over all of P–T space except at the lowest temperatures and highest pressures. Disregarding the discrepancy in the upper left of the diagram, the maximum difference in temperature between the EQ and MDF models for a given value of K_D is around 10 °C. At 600 °C, 1 GPa the compositions of garnet and biotite differ somewhat in the two models, but the ratio $(Fe/Mg)_{Grt}/(Fe/Mg)_{Bt}$ is relatively similar (7.681 versus 7.451) and the difference does not propagate into a large difference in temperature that would be inferred through application of the garnet-biotite thermometer. That is, growth of garnet following the MDF equations rather than the equilibrium equations does not greatly affect the calculated temperature using a thermometer based on the Fe/Mg ratios of garnet and biotite. This result is perhaps not surprising because the MDF equations ensure Fe-Mg partitioning equilibrium between garnet and other phases.

Table 4
Comparison of garnet and plagioclase compositions from the EQ and MDF models at 600 °C, 1 GPa and mineral compositions in sample TM-626.

	EQ model	MDF model
Xprp	0.088	0.046
Xalm	0.754	0.552
Xsps	0.079	0.314
Xgrs	0.079	0.088
Grt Fe/(Fe + Mg)	0.895	0.923
Bt Fe/(Fe + Mg)	0.526	0.620
Xan	0.128	0.221
(Fe/Mg)Grt/(Fe/Mg)Bt	7.681	7.415
(Xan/Xgrs)^3	4.25	15.84

The results of a similar pair of calculations for the garnet-plagioclase-muscovite-biotite barometer (calibration of Hodges and Crowley, 1985), however, reveal significant differences in the P–T locations of the equilibrium constant for this barometer (Fig. 6b):

$$K_{Eq} = \frac{a_{grs} a_{prp} a_{ms}}{a_{phl} a_{ano}^3} \quad (4)$$

here written in terms of Mg end-member components. With phase compositions controlled by equilibrium relations, the isopleths of the equilibrium constant are quite flat (black lines in Fig. 6b). However, with phase compositions controlled by the MDF relationships, the isopleths are considerably steeper (red lines in Fig. 6b) than with the

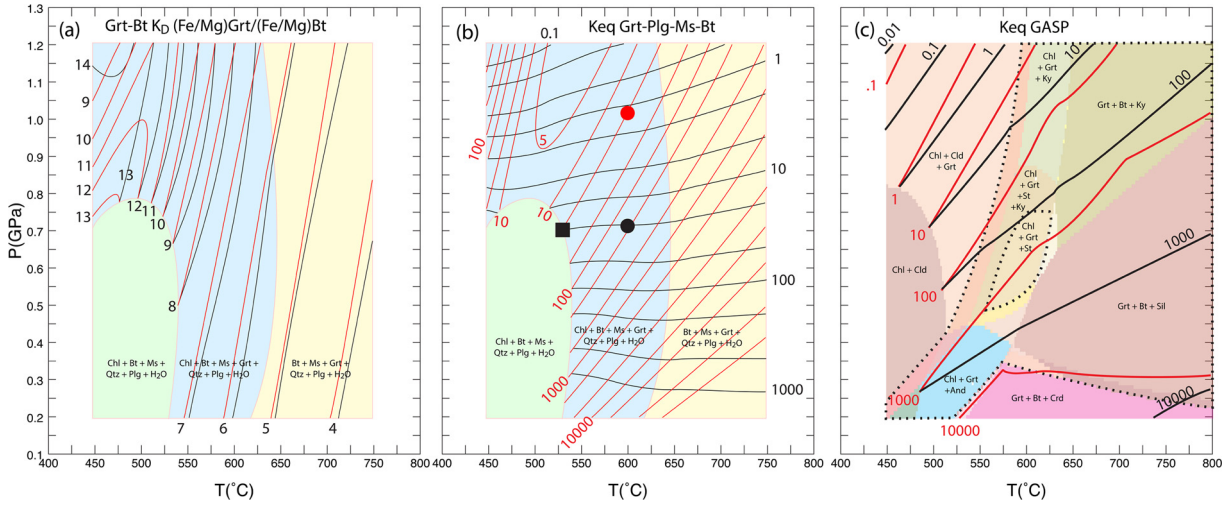

Fig. 6. Equilibrium MAD P–T diagrams for the MnNCKFMASH system for two bulk compositions. (a) and (b) are calculated for the bulk composition of TM-626 and (c) is calculated for a hypothetical high-Al bulk composition. (a) Diagram contoured with values of Grt-Bt KD. (b) Diagram contoured with values of Keq for the equilibrium Grt-Plg-Ms-Bt (GPMB). (c) Diagram contoured for the equilibrium constant for the Grt-Plg-AlSi (GASP) barometer. Black contours are calculated from equilibrium garnet compositions, red contours are calculated from MDF garnet compositions. Note the similarity in contours for the Grt-Bt thermometer but the significant difference for the GPMB and GASP barometers. Dotted lines in (c) outline the fields where an aluminosilicate is stable, but contours are drawn in all garnet-bearing fields to better show the relationship between the two sets of contours.

equilibrium formulation (black lines). The consequences of this difference are substantial if it is not known whether a garnet nucleated and grew under near-equilibrium conditions or only after considerable overstepping. Consider, for example, a garnet-bearing sample with a garnet core and plagioclase composition that yielded a value of the equilibrium constant of 20. Assuming equilibrium nucleation, the interpretation of this calculation would place the garnet core at the garnet isograd at around 530 °C, 0.7 GPa (black square in Fig. 6b). Even if independent constraint on the temperature of the garnet core were available, the inferred pressure would still be around 0.7 GPa (e.g. black circle in Fig. 6b). However, if the garnet nucleated only after considerable overstepping then the core P–T conditions would fall along the red isopleth for the same value of the equilibrium constant, for example at around 600 °C, 1.0 GPa (red circle in Fig. 6b). If the peak metamorphic conditions were inferred to be around 600 °C, 1.0 GPa, then it is clear that the prograde P–T path inferred from garnet zoning varies significantly depending on whether equilibrium is assumed.

A similar set of calculations for the garnet-plagioclase-aluminosilicate (GASP) barometer are presented in Fig. 6c in which the ratio

$$K_{Eq} = \frac{a_{grs}}{a_{an}^3} \tag{5}$$

has been contoured for both the EQ and MDF models. The differences in slopes is not as pronounced as with the GPMB barometer, but the same generalization holds true: namely, the P–T conditions inferred from the garnet core are strongly dependent on the degree of overstepping.

The differences in the results of barometric calculations for the EQ and MDF models can be understood by comparing the controlling activity constants for grossular and anorthite components in the two models. The equilibrium compositions are controlled by the constants (4) or (5). With compositions constrained by the MDF relations, however, the grossular and anorthite components are controlled by relations such as

$$K = \frac{a_{grs} a_{phl}^3 a_{ms}^3 a_{qtz}^{12}}{a_{prp} a_{an}^3 a_{cel}^6}$$

or

$$K = \frac{a_{grs} a_{cel}^3}{a_{prp} a_{an}^3 a_{ms}^3}$$

Note that the ratio of grossular to anorthite appears in both the EQ and MDF relations, but the MDF constant contains the ratio of the activities of grossular to pyrope in both cases.

6.1. Application

Results of calculations on four samples from the Connecticut Valley Trough, New England, are presented as representative of the results to be expected by applying the above reasoning to natural samples. These samples were chosen because the metamorphic evolution of the terrane is relatively well-known (e.g. Menard and Spear, 1994; Wolfe and Spear, 2018) and the rocks have only experienced a single Barrovian metamorphic event.

Four curves are shown in Fig. 7 for each sample. The inferred P–T conditions for garnet nucleation (black square) are constrained by the QuiG barometry (dashed-dotted line), garnet-biotite Fe-Mg exchange thermometry, zirconium in rutile thermometry, and pseudosection analysis following the methods described in Wolfe and Spear (2017, 2018). Results of application of the garnet-plagioclase-muscovite-biotite (GPMB) barometer (calibration of Hodges and Crowley, 1985) using the measured garnet and plagioclase core and matrix muscovite and biotite compositions are shown as solid lines. In addition, two sets of model calculations are also shown. For the equilibrium calculation (EQ model), the compositions of garnet, plagioclase, chlorite, muscovite and biotite at the inferred conditions of garnet nucleation (black square) were calculated using Program Gibbs and the SPaC thermodynamic dataset (Spear and Pyle, 2010) and the measured bulk composition of the sample. For the MDF model calculations, the same P–T conditions, thermodynamic data set, and equilibrium assumptions were used for all phases except garnet, and the composition of garnet was calculated using the MDF approach described above. The GPMB barometer was then applied to each set of mineral compositions and the results plotted as dashed (EQ model) and dotted (MDF model) lines.

The results for sample OW-18 (Fig. 7a) are quite consistent with the theoretical results described above and in Fig. 6. The curve for the GPMB barometer using measured garnet and plagioclase core and matrix biotite and muscovite compositions (solid line) lies nearly coincident with the theoretical calculations using the MDF model (dotted line). The results for sample TM-626 are similar to those for OW-19 except the GPMB curves using the measured compositions (black lines) fall 0.1-0.2 GPa above that for the MDF model. For sample OW-19, the GPMB barometer results fall 0.2-0.3 GPa above the predicted MDF model and for sample OW-5c (which is the only epidote-bearing sample examined in this study), the measured compositions yield a barometric curve (black line) that lies nearly 0.5 GPa above the MDF model. Fortuitously, the barometric results for the measured compositions of the garnet and plagioclase cores for samples OW-19 and OW-5c also fall very close to the inferred conditions of garnet nucleation (black square).

7. Discussion

The results shown in Fig. 7 indicate that at least some samples follow the theoretical analysis of overstepping and the MDF calculations, but others do not. In fact, the compositions of phases in samples OW-19 and OW-5c appear to be more consistent with equilibrium crystallization of the garnet core and coexisting plagioclase than with the overstepped (MDF) model. Whereas this is a tempting conclusion to draw, it is not believed to be correct for the simple fact that, in equilibrium, there is no driving force for garnet to grow, thus creating a logical inconsistency. Indeed, the result of previous work on these samples (Wolfe and Spear, 2017, 2018) indicate that the garnet grew under nearly isothermal and isobaric conditions. Of course, there are mechanisms to drive garnet growth such as the influx of a CO_2-rich fluid, but these are considered ad-hoc. Rather, it is believed that the range of results displayed in Fig. 7 are the consequence of the local effective bulk composition during garnet growth.

As demonstrated by Spear and Wolfe (2018), the effective bulk composition (EBC) during the growth of the garnet core in these and other samples is not the same as the measured bulk rock composition (e.g. Fig. 2). Those calculations only considered variations in the FeO, MnO, and CaO content of the EBC required to produce the measured garnet core composition using the MDF calculations. The GPMB barometer, however, also assumes equilibrium with plagioclase. Specifically, the calculations presented in Fig. 7 assume that the Na_2O content of the EBC (not considered by Spear and Wolfe, 2018) was that measured for the whole-rock. Plagioclase cannot undergo significant lattice diffusion at the P–T conditions of these samples and thus the CaO required to grow garnet must come from recrystallization of existing plagioclase. In the epidote-free samples examined (OW-18, TM-626, and OW-19), plagioclase is invariably zoned from calcic cores to more sodic rims. Only in the epidote-bearing sample (OW-5c) is plagioclase zoned towards more calcic rims. In either case, in order for plagioclase to recrystallize with a new composition, Na must be sequestered from the old plagioclase into the new plagioclase. This must result in an EBC in the vicinity of garnet that is lower in Na than measured in the whole-rock analysis. To test this hypothesis, consider the results for sample TM-626. The measured plagioclase composition ranges from An_{14}-An_{11}. The measure whole-rock Na_2O content is 1.25 wt% and the calculated equilibrium plagioclase composition with this Na_2O content is An_{12}. In

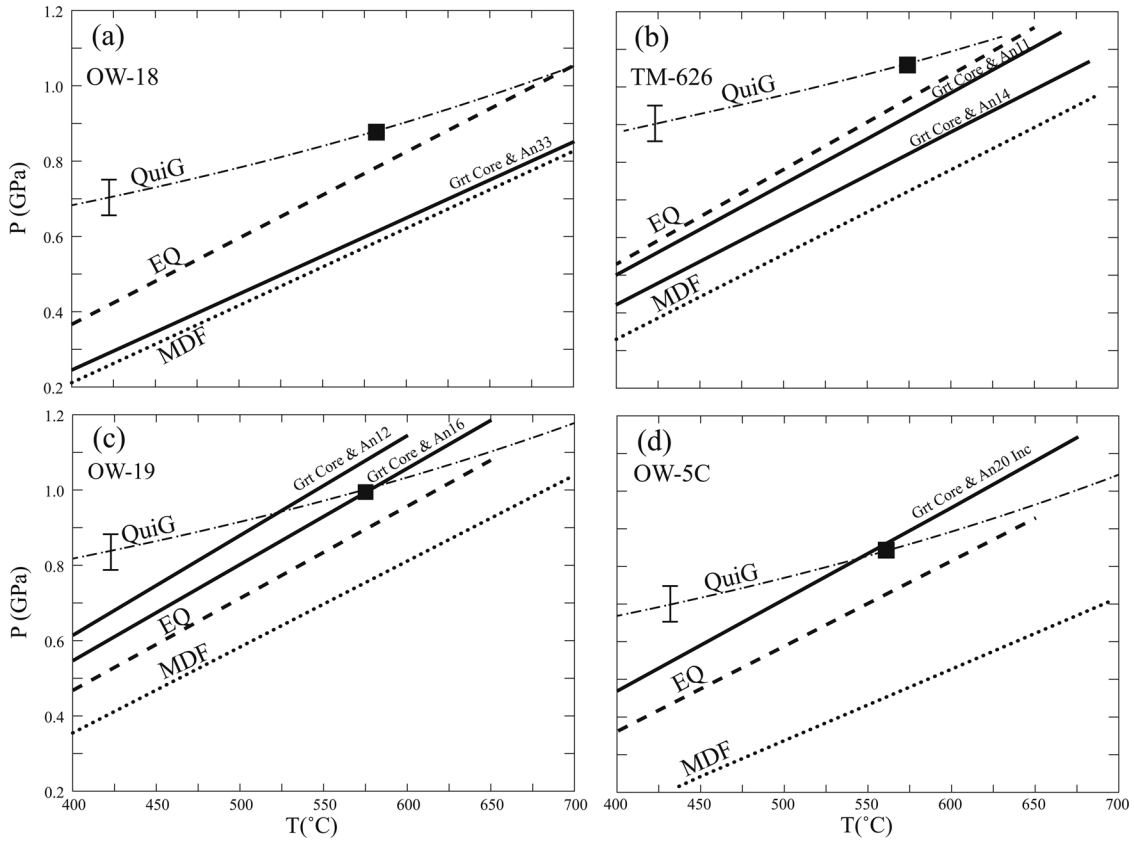

Fig. 7. P–T diagrams showing the results of barometric calculations for four samples from the Connecticut Valley Terrane in western New England. Inferred P–T conditions of garnet core growth are shown by black square. Garnet-plagioclase-muscovite-biotite barometry using measured garnet and plagioclase core and matrix biotite and muscovite compositions are shown with solid lines. The results of the model thermobarometry calculations using calculated garnet, plagioclase, biotite and muscovite compositions at conditions of the square are shown as dotted (equilibrium model) and dashed (MDF model) lines. Results of QuiG barometry are shown with dot-dashed lines.

order for the MDF curve to fall on the measured GPMB barometer, however, the plagioclase composition would need to be around An_{22}, which would require an EBC in the vicinity of garnet with Na_2O content of 0.30 wt%. Consequently, it is concluded that the reason the measured GPMB curves fall above the calculated MDF curves for samples TM-626, OW-19, and OW-5c is that the effective Na_2O content in the vicinity of garnet is actually considerably lower than that measured in the whole-rock analysis because Na_2O is sequestered by recrystallizing plagioclase.

These results suggest that the EBC in a recrystallizing schist is controlled very locally and may be highly variable from place to place in a rock. As phrased by Putnis and Austrheim (2010), "…every metamorphic reaction is metasomatic on a local scale." This appears to be true whether reactions are driven by fluid influx (e.g. Putnis and Austrheim, 2010) or by significant overstepping.

The above calculations also demonstrate that if the chemical zoning of garnet grown isothermally and isobarically is used in equilibrium calculations, P–T paths deduced from analysis of this zoning will fortuitously appear to involve loading with or without an increase in temperature. Inasmuch as P–T paths involving loading and heating are to be expected from crustal thickening tectonic scenarios, these paths are of considerable interest to petrologists. However, the results of the present study raise the somewhat unwelcome specter that many of the published P–T paths based on chemical zoning in garnet using either equilibrium thermobarometry or intersecting isopleths may be in error.

It is important to recognize that the quantitative conclusions of this contribution are based on the assumption that the MDF model accurately recovers the composition of garnet nucleating and growing out of equilibrium with its matrix assemblage. The MDF model (also referred to as the parallel tangent method) has been applied to the nucleation of a phase (e.g. Thompson and Spaepen, 1983; Hillert, 2008; Pattison et al., 2011; Gaidies et al., 2011; Spear et al., 2014) and to the growth of a garnet porphyroblast (e.g. Spear, 2017). However, application of the parallel tangent model to the growth of phases has been questioned by Hillert (1999) and Hillert and Rettenmayr (2003). The energetics of a growing porphyroblast in a solid matrix are not the same as those described by these authors, who were analyzing phases growing from an aqueous solution or melt. However, these studies do raise the question as to the correct formulation of the governing equations for a porphyroblast growing out of equilibrium. Nevertheless, a phase growing out of equilibrium cannot be governed by the same equations as a phase growing in equilibrium, so application of equilibrium approaches to phases nucleating and growing after considerable overstepping must be modified.

It is also important to note that the principal observational data motivating this study are the results from the application of QuiG barometry. A major conclusion from the application of QuiG barometry to garnet nucleation and growth is that garnet nucleates only after considerable overstepping in temperature and pressure and grows nearly isothermally and isobarically at the metamorphic peak (e.g. Spear et al., 2014; Castro and Spear, 2016; Wolfe and Spear, 2018).

One possibility that would invalidate the conclusions drawn from the QuiG results is if there is a mechanism by which quartz inclusions could readjust their internal pressures during prograde metamorphism. Whereas there are mechanisms by which internal pressures on quartz inclusions can be decreased from their initial maximum values such as cracking of the garnet host or other inelastic strain, a mechanism that would result in an increase in the pressure of a quartz inclusion is more

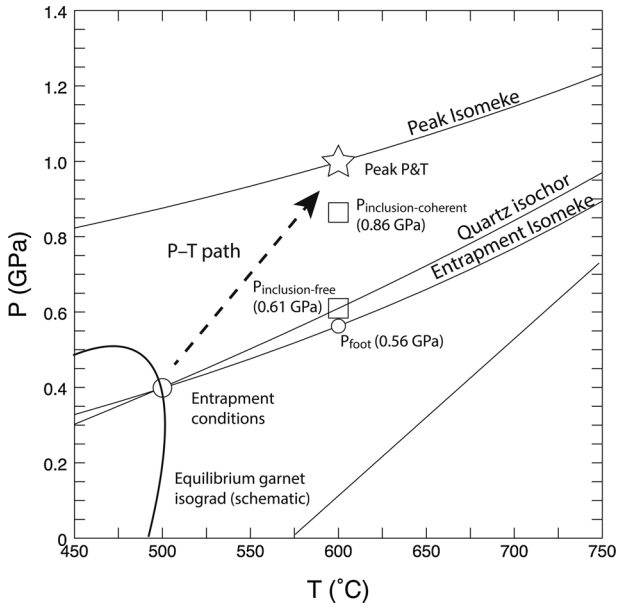

Fig. 8. P–T diagram showing hypothetical scenario where quartz is entrapped in garnet at the garnet isograd and then experiences peak P–T conditions at 600 °C, 1 GPa. At these peak conditions, the pressure on the inclusion is 0.86 GPa, which exerts extensional strain on the garnet. The two isomekes are those for the entrapment and peak conditions. The quartz isochore is the constant volume line for quartz that passes through the entrapment P–T conditions. P_{foot} is the pressure along the entrapment isomeke at the peak T. $P_{inclusion\text{-}coherent}$ is the pressure on the inclusion under extensional stress from the host and $P_{inclusion\text{-}free}$ is the pressure on the inclusion if it detaches from the host. Note that the $P_{inclusion\text{-}coherent}$ is less than the peak P so any modification of the inclusion pressure due to plastic deformation in the host should result in the QuiG pressure being lower than the peak pressure.

difficult to envision. However, if such a mechanism did exist then it could, in theory, be possible that a quartz grain entrapped in garnet during initial garnet growth at or very near the equilibrium garnet isograd might experience an increase in internal pressure up to the peak metamorphic P–T conditions. If the pressure of such an inclusion were preserved during exhumation then application of QuiG barometry would yield the apparent result that the garnet nucleated near the peak P–T conditions whereas, in fact, the garnet had nucleated near the equilibrium isograd and the inclusion pressure was reset near the metamorphic peak.

As an example, consider a rock in which a quartz grain is encapsulated in garnet at 500 °C, 0.4 GPa and the rock is then subjected to peak P–T conditions of 600 °C, 10 kb. The question to be addressed is: what pressure will be felt by the quartz grain at the peak conditions and what mechanism, if any, can be envisioned that would result in the inclusion pressure being reset to the peak pressure? This calculation can be done by modification of the procedure described in detail by Angel et al., 2017 (Fig. 8). First, the isomeke for the entrapment conditions is calculated and P_{foot} determined along this isomeke at the peak temperature. Then $P_{inclusion}$ is calculated from the thermoelastic model of Guiraud and Powell (2006). These calculations yield a $P_{inclusion}$ of 0.8642 GPa at the peak metamorphic conditions.

The quartz inclusion has a lower pressure than the peak pressure so the garnet host experiences extensional strain surrounding the inclusion, provided the quartz-garnet grain boundary remains coherent. If the extensional strain in garnet is relieved by, say, plastic deformation, then it is conceivable that the pressure on the quartz inclusion could reach that of the peak pressure. However, observations of natural samples in which quartz has been entrapped in garnet at low pressure reveals extensional strains in the garnet host in excess of 1500 bars (Wolfe and Spear, 2017, and unpublished data). These samples reveal preservation of the extensional strains in garnet during cooling from over 600 °C is possible, so it is considered unlikely that relaxation of the extensional strain in scenarios such as described above will occur.

Alternatively, if the grain boundary detaches, the extensional strain in the garnet would be released and the quartz crystal would sit in a void space at indeterminate pressure. In this case, there is no driving force for garnet to deform. In addition, it is unlikely that mass diffusion could result in filling the void space with either additional SiO_2 or components to make additional garnet. If new garnet were produced in such void space, it would likely have a different composition than the adjacent garnet an no such compositional heterogeneities have ever been detected.

In summary, although it is possible that the QuiG barometer could be reset to the peak metamorphic conditions, there is no direct evidence that this has occurred and no mechanism has been proposed where this is feasible. A possible resolution to this uncertainty is to find a sample in which garnet has grown with quartz inclusions at low pressure and then continued to grow during a second event at high pressure. If the garnet core preserved the early, low pressure growth history this would strongly support the robustness of QuiG. Additionally, experiments in which this scenario was created in the lab could also verify that QuiG maintains the pressure of garnet formation. In any case, this is a topic worthy of future research.

8. Conclusions

The main conclusions of this work are these:

(a) The chemical zoning in garnet grown isothermally and isobarically after overstepping is nearly identical to the chemical zoning calculated along a P–T path under successive equilibrium conditions (see also Spear, 2017).
(b) Calculations of P–T paths using intersecting garnet isopleths from isothermally and isobarically grown garnet in which it is assumed that garnet grew under equilibrium conditions will yield apparent, but incorrect, paths characterized by loading with minor heating.
(c) Fe-Mg exchange geothermometry on garnet cores and rims yield results consistent with the conditions of garnet growth.
(d) Garnet-plagioclase geobarometry using garnet + plagioclase cores and rims yields apparent, but incorrect, P–T paths characterized by nearly isothermal loading.

These results suggest that many published studies in which P–T paths have been inferred from garnet zoning assuming growth along successive equilibrium stages need to be reevaluated. Key outstanding questions revealed by this work include (a) the extent to which QuiG barometry accurately records the conditions of garnet nucleation and growth; (b) the accuracy of the thermodynamic data and activity models used in calculations; (c) the appropriate governing equations to use when a crystal grows after overstepping; and (d) the extent to which the effective bulk composition varies over short distances during metamorphic recrystallization and how this affects the compositions of the reacting phases.

Declaration of Competing Interest

The authors declare that they have no known competing financial interests or personal relationships that could have appeared to influence the work reported in this paper.

The authors declare the following financial interests/personal relationships which may be considered as potential competing interests:

Acknowledgments

This work has been supported by grants from the National Science Foundation1447468 and 1750674 (to Spear) and the Edward P.

Hamilton Distinguished Professor of Science Education Chair (Rensselaer).

References

Angel, R.J., Mazzucchelli, M.L., Alvaro, M., Nestola, F., 2017. EosFit-Pinc: a simple GUI for host-inclusion elastic barometry. Am. Mineral. 102, 1957–1960.

Ashley, K.T., Caddick, M.J., Steele-MacInnis, M.J., Bodnar, R.J., Dragovic, B., 2014. Geothermobarometric history of subduction recorded by quartz inclusions in garnet. Geochem. Geophys. Geosystems 15 (2), 350–360.

Berman, R.G., 1988. Internally-consistent thermodynamic data for minerals in the system Na_2O - K_2O - CaO - MgO - FeO - Fe_2O_3 - Al_2O_3 - SiO_2 - TiO_2 - H_2O - CO_2. J. Petrol. 29, 445–522.

Berman, R.G., 1990. Mixing properties of Ca-Mg-Fe-Mn garnets. Am. Mineral. 75, 328–344.

Carlson, W.D., 1989. The significance of intergranular diffusion to the mechanisms and kinetics of porphyroblast crystallization. Contrib. Mineral. Petrol. 103, 1–24.

Carlson, W.D., 1991. Competitive diffusion-controlled growth of porphyroblasts. Mineral. Mag. 55, 317–330.

Carlson, W.D., 2002. Scales of disequilibrium and rates of equilibration during metamorphism. Am. Mineral. 87, 185–204.

Carmichael, D.M., 1969. On the mechanism of prograde metamorphic reactions in quartz-bearing pelitic rocks. Contrib. Mineral. Petrol. 20, 244–267.

Castro, A.E., Spear, F.S., 2016. Reaction overstepping and reevaluation of the peak P-T conditions of the blueschist unit sifnos, Greece: implications for the cyclades subduction zone. Int. Geol. Rev. 59, 548–562.

Dachs, E., Geiger, C.A., Withers, A.C., Essene, E.J., 2009. A calorimetric investigation of spessartine: vibrational and magnetic heat capacity. Geochim. Cosmochim. Acta 73, 3393–3409.

Dragovic, B., Samanta, L.M., Baxter, E.F., Selverstone, J., 2012. Using garnet to constrain the duration and rate of water-releasing metamorphic reactions during subduction: an example from Sifnos, Greece. Chem. Geol. 314, 9–22.

Gaidies, F., Abart, R., De Capitani, C., Connolly, J.A.D., Reusser, E., 2006. Characterization of polymetamorphism in the Austroalpine basement east of the Tauern Window using garnet isopleth thermobarometry. J. Metamorph. Geol. 24, 451–475.

Gaidies, F., Krenn, E., de Capitani, C., Abart, R., 2008. Coupling forward modelling of garnet growth with monazite geochronology: an application to the Rappold Complex (Austroalpine crystalline basement). J. Metamorph. Geol. 26, 775–793.

Gaidies, F., Pattison, D.R.M., de Capitani, C., 2011. Toward a quantitative model of metamorphic nucleation and growth. Contrib. Mineral. Petrol. 162 (5), 975–993.

Gaidies, F., Petley-Ragan, A., Chakraborty, S., Dasgupta, S., Jones, P., 2015. Constraining the conditions of Barrovian metamorphism in Sikkim, India: P–t–t paths of garnet crystallization in the Lesser Himalayan Belt. J. Metamorph. Geol. 33, 23–44.

George, F.R., Gaidies, F., 2017. Characterisation of a garnet population from the Sikkim Himalaya: insights into the rates and mechanisms of porphyroblast crystallisation. Contrib. Mineral. Petrol. 172.

Guiraud, M., Powell, R., 2006. P–V–T relationships and mineral equilibria in inclusions in minerals. Earth Planet. Sci. Lett. 244 (3-4), 683–694.

Hillert, M., 1999. Solute drag, solute trapping and diffusional dissipation of Gibbs energy. Acta Mater. 47, 4481–4505.

Hillert, M., 2008. Phase Equilibria, Phase Diagrams and Phase Transformations: Their Thermodynamic Basis. Cambridge University Press, Cambridge.

Hillert, M., Rettenmayr, M., 2003. Deviation from local equilibrium at migrating phase interfaces. Acta Mater. 51, 2803–2809.

Hodges, K.V., Crowley, P.D., 1985. Error estimation and empirical geothermobarometry for pelitic systems. Am. Mineral. 70, 702–709.

Holland, T.J.B., Powell, R., 1998. An internally-consistent thermodynamic dataset for phases of petrological interest. J. Metamorph. Geol. 16, 309–343.

Holland, T.J.B., Powell, R., 2011. An improved and extended internally consistent thermodynamic dataset for phases of petrological interest, involving a new equations of state for solids. J. Metamorph. Geol. 29, 333–383.

Hollister, L.S., 1969. Contact metamorhpism in the Kwoiek Area of British Columbia: an end member of the metamorphic process. Geol. Soc. Am. Bull. 80, 2465–2494.

Lanari, P., Duesterhoeft, E., 2019. Modeling metamorphic rocks using equilibrium thermodynamics and internally consistent databases: past achievements, problems and perspectives. J. Petrol. 60, 19–56.

Menard, T., Spear, F.S., 1994. Metamorphic P-T paths from calcic pelitic schists from the Strafford Dome, Vermont. J. Metamorph. Geol. 12, 811–826.

Moynihan, D.P., Pattison, D.R.M., 2013. An automated method for the calculation of P-T paths from garnet zoning, with application to metapelitic schist from the Kootenay Arc, British Columbia, Canada. J. Metamorph. Geol. 31 (5), 525–548.

Palin, R.M., Weller, O.M., Waters, D.J., Dyck, B., 2016. Quantifying geological uncertainty in metamorphic phase equilibria modeling: a Monte Carlo assessment and implications for tectonic interpretations. Geosci. Front. 7, 591–607.

Pattison, D.R.M., de Capitani, C., Gaidies, F., 2011. Petrological consequences of variations in metamorphic reaction affinity. J. Metamorph. Geol. 29 (9), 953–977.

Pattison, D.R.M., DeBuhr, C.L., 2015. Petrology of metapelites in the Bugaboo aureole, British Columbia, Canada. J. Metamorph. Geol. 33, 437–462.

Pattison, D.R.M., Tinkham, D.K., 2009. Interplay between equilibrium and kinetics in prograde metamorphism of pelites: an example from the Nelson aureole, British Columbia. J. Metamorph. Geol. 27, 249–279.

Putnis, A., Austrheim, H., 2010. Fluid-induced processes: metasomatism and metamorphism. Geofluids 10, 254–269.

Spear, F.S., 1993. Metamorphic Phase Equilibria and Pressure-Temperature-Time Paths. Mineralogical Society of America, Washington, D. C.

Spear, F.S., 2017. Garnet growth after overstepping. Chem. Geol. 466, 491–499.

Spear, F.S., Pattison, D.R.M., 2017. The implications of overstepping for metamorphic assemblage diagrams (MADs). Chem. Geol. 457, 38–46.

Spear, F.S., Pyle, J.M., 2010. Theoretical modeling of monazite growth in a low-Ca metapelite. Chem. Geol. 266, 218–230.

Spear, F.S., Thomas, J.B., Hallett, B.W., 2014. Overstepping the garnet isograd: a comparison of QuiG barometry and thermodynamic modeling. Contrib. Mineral. Petrol. 168 (3), 1–15.

Spear, F.S., Wolfe, O.M., 2018. Evaluation of the effective bulk composition (EBC) during growth of garnet. Chem. Geol. 491, 39–47.

St-Onge, M.R., Davis, W.J., 2017. Wopmay orogen revisited: phase equilibria modeling, detrital zircon geochronology, and U–Pb monazite dating of a regional Buchan-type metamorphic sequence. Geol. Soc. Am. Bull. 130, 678–704.

Thomas, J.B., Spear, F.S., 2018. Experimental study of quartz inclusions in garnet at pressures up to 3.0 GPa: evaluating validity of the quartz-in-garnet inclusion elastic thermobarometer. Contrib. Mineral. Petrol. 173, 14.

Thompson, C.V., Spaepen, F., 1983. Homogeneous crystal nucleation in binary metallic melts. Acta Metall. 31, 2021–2027.

Thompson Jr, J.B., 1982. Composition space: an algebraic and geometric approach. In: Ferry, J.M. (Ed.), Characterization of Metamorphism through Mineral Equilibria. Mineralogical Society of America, Washington, D. C, pp. 1–31 Reviews in Mineralogy.

Tinkham, D.K., Ghent, E.D., 2005a. Estimating P–T conditions of garnet growth with isochemical phase-diagram sections and the problem of effective bulk-composition. Can. Mineral. 43, 35–50.

Tinkham, D.K., Ghent, E.D., 2005b. XRMapAnal: a program for analysis of quantitative X-ray maps. Am. Mineral. 90, 737–744.

Waters, D.J., Lovegrove, D.P., 2002. Assessing the extent of disequilibrium and overstepping of prograde metamorphic reactions in metapelites from the Bushveld Complex aureole, South Africa. J. Metamorph. Geol. 20 (1), 135–149.

White, R.W., Powell, R., Holland, T.J.B., Johnson, T.E., Green, E.C.R., 2014a. New mineral activity-composition relations for thermodynamic calculations in metapelitic systems. J. Metamorph. Geol. 32 (3), 261–286.

White, R.W., Powell, R., Johnson, T.E., 2014b. The effect of Mn on mineral stability in metapelites revisited: new a-x relations for manganese-bearing minerals. J. Metamorph. Geol. 32 (8), 809–828.

Wilbur, D.E., Ague, J.J., 2006. Chemical disequilibrium during garnet growth: monte Carlo simulations of natural crystal morphologies. Geology 34 (8), 689–692.

Wolfe, O.M., Spear, F.S., 2017. Textural Constraints on the P–T Conditions of Garnet Nucleation and Appearance of Rutile in Connecticut Valley Synclinorium VT Metapelites, and Cooling Rates From Peak T. Geological Society of America, Seattle, WA.

Wolfe, O.M., Spear, F.S., 2018. Determining the amount of overstepping required to nucleate garnet during Barrovian regional metamorphism, Connecticut Valley Synclinorium. J. Metamorph. Geol. 36, 79–94.